Catalysis Today 146 (2009) 378–385

Contents lists available at ScienceDirect

Catalysis Today

journal homepage: www.elsevier.com/locate/cattod

Electrochemically stable gold nanoclusters in HOPG nanopits

M. Limat [a], G. Fóti [a], M. Hugentobler [b], R. Stephan [b,1], W. Harbich [b,*]

[a] Electrochemical Engineering Group, École Polytechnique Fédérale de Lausanne, 1015 Lausanne, Switzerland
[b] Institut de Physique des Nanostructures, École Polytechnique Fédérale de Lausanne, 1015 Lausanne, Switzerland

ARTICLE INFO

Article history:
Available online 28 July 2009

Keywords:
Gold nanoparticles
Highly oriented pyrolytic graphite
Evaporation deposition
Heat treatment
Electrochemical stability
Electrocatalysis

ABSTRACT

Gold nanoparticles on highly oriented pyrolytic graphite (HOPG) electrodes are synthesized. They are stabilized in nanosized pits of well defined depth in the graphite surface. These pits are created by energetic cluster impact followed by etching under a well controlled oxygen atmosphere. We succeeded in the preparation of highly dispersed and stable Au electrodes with gold particles with a mean diameter smaller than 5 nm. The stability of the gold nanostructures for electrochemical applications has been tested by performing cyclic voltammetric measurements in 0.5 M H_2SO_4. While conventionally prepared sputter deposited electrodes show highly unstable structures in this size range, Au clusters stabilized in the nanosized containers are stable.

1. Introduction

Gold nanoparticles have attracted considerable interest in the past decade due to their geometrical, electronic and chemical properties which differ drastically from those of bulk materials [1,22]. Gold is known as an extremely stable and established weak chemisorber, therefore a poor catalyst. The seminal work of Haruta [23,22] has shown that gold shows surprisingly strong catalytic activity when dispersed as nanoparticles on a substrate. Goodman and coworkers [39] clearly delimited the size range to be below 5 nm. Since then a new field opened up known as nanocatalysis by gold [24]. Gold exhibits remarkable electrocatalytic activity, higher than that of other transition metals towards many reactions like catalytic hydrogenation of unsaturated alcohols and aldehydes [35], CO oxidation [4,20–22], selective hydrocarbon oxidation [26] and O_2 reduction [14,41]. The detailed mechanisms of this exceptional activity are not well understood yet. Numerous studies have been performed over the last years to better understand the electrochemical properties of gold nanoparticles in heterogeneous catalysis and surface electrochemistry. Gold catalyst systems, i.e. supported Au nanoparticles, can be used for applications in pollution control, chemical processing and fuel cells. It is not only the promising technical performance gold catalysts can provide [9], but also an economical challenge, because of the lower price of gold against platinum, which is the currently used catalyst.

In the perspective to prepare stable electrocatalysts, several groups investigated the electrocatalytic activity of metallic nanoparticles like platinum [33,37], silver and gold [41,33] deposited on boron-doped diamond (BDD) electrodes. In our research group, a new technique for the preparation of stable and applicable gold nanoparticles supported on boron doped diamond has been developed [33]. Gold deposits have been assumed to agglomerate at specific actives sites of the BDD film corresponding to the surface defects. Ultrafine Gold particles on carbon substrates (glassy carbon) have first been considered as substrates by Yahikozawa et al. [40] and Tateishi et al [38]. Highly oriented pyrolytic graphite (HOPG) has also to be considered as a support because it is an attractive electrode material due to its wide potential window in aqueous media with a low background current. Furthermore this support is inert and chemically stable [31]. HOPG electrodes have been widely investigated due to their strong anisotropic surface properties [3].

The basal plane of HOPG having all carbon bonds saturated is extremely inert with a small energy barrier for adatom diffusion. Consequently it is difficult to stabilize nanoparticles on the surface terraces and aggregation takes place at monoatomic step edges [11,12,15,18]. This results in a strongly anisotropic distribution of nanoparticles on the surface like metallic chains [12], a difficult size control and even more important in a small particle density. A possible way to stabilize very small nanostructures is to pin the particles via the creation of defects to the surface [7,8,30,10,17,19]. However these structures although to some extent stable under vacuum conditions at room temperature alter upon exposure to atmospheric conditions or when immersed in solutions. Instead of

---

* Corresponding author.
E-mail address: wolfgang.harbich@epfl.ch (W. Harbich).

[1] Present address: Institut de Science des Matériaux de Mulhouse, (IS2M) - LRC CNRS 7228 Université de Haute-Alsace, 4 rue des frères Lumière, 68093 Mulhouse Cedex, France.

0920-5861/$ – see front matter © 2009 Elsevier B.V. All rights reserved.
doi:10.1016/j.cattod.2009.06.021

stabilizing the particles by partial implantation of the cluster atoms one can imagine to keep them in place on strongly nanostructured surfaces.

HOPG is a model candidate for such type of substrates. Kappes and coworkers [5,6] where the first to create controlled nanosize pits in ion bombarded HOPG. These pits could be created by selective etching of defects introduced by ion beam impact. Several groups, including the authors have followed this idea [16,25,2,27,32,34,36].

In the following we describe the application of this method to the preparation of stable HOPG electrodes for electrochemical processes. Very small gold clusters ($\leq$5 nm) are fixed in these nanopits and show to be surprisingly stable. The nanosized gold deposits are characterized by scanning tunneling microscopy (STM), scanning electron microscopy (SEM) and cyclic voltammetry (CV).

2. Phenomenological description

The preparation of highly dispersed nanosized particles on a substrate by physical vapor deposition or sputtering involves two basic processes: nucleation and particle growth. These processes strongly depend on the bond energy of the contributing atoms to the surface and the surface corrugation for diffusion and often take place simultaneously. Suitably chosen experimental conditions may favor one process over the other hence one may tailor the granulometric properties of the dispersion.

Electrochemical deposition processes are mostly characterized by growth rather than nucleation leading to the formation of very large clusters without completion of the first monolayer. As a consequence, the size of the clusters is difficult to control and exceeds easily the desired range of some tens of nanometers. Aiming to prepare metal nanoparticles of tailored size less than 10 nm and well adhered to the HOPG substrate we separate nucleation and particle growth. The process, sketched in Fig. 1, consists of three consecutive steps: (1) implantation of gold clusters (Au_5 in this case) at a well defined impact energy on the HOPG surface to create the desired number of defects, (2) etching of these pits under controlled temperature and oxygen atmosphere, and (3) gold deposition by evaporation onto the substrate at 400 °C. The application of this method is limited to small surface loading of the deposited material, typically not exceeding a few monolayer equivalent but is perfectly suited to produce very small supported clusters.

An atomically clean HOPG surface containing only a small fraction of edge planes ($<5\%$) is exposed to Au_5 clusters with an appropriate kinetic energy ($\sim$3 keV). The bombardment involves permanent displacements of surface and subsurface carbon atoms. These displacements (defects) create dangling bonds which serve as oxidation sites for the successive etching step. Au_5 clusters have been chosen for their size is large enough to guarantee a well defined defect depth (3–4 monolayers) [36] and to avoid implantation of other metals than the desired electrode material. Control of the defect density is easily achieved via the bombarding time.

During the second step the defects are opened into nanosized pits. The carbon-oxygen reaction is highly dependent on the nature of the carbon sites. Carbon atoms with saturated bonds (the ones in the basal plane) are much more inert than the ones with dangling bonds. At temperatures below 700 °C, oxidation is initiated mainly at defects on the basal plane, or edge atoms on monoatomic steps while intact basal plane atoms remain unaffected. The oxidation removes carbon atoms from the basal plane of graphite and creates new vacancies. This process continues until the penetration depth of defect production is reached. The diameter of the pit however continues to grow and is largely dependent on the oxidation time.

The third step consists in evaporation of gold under high vacuum conditions ($p \approx 10^{-4}$ Pa). The carbon electrode is heated to 400 °C which confers sufficient energy to the gold atoms to migrate into the pits. The number of individual nanoparticles depends on the pit density while the cluster size is defined by the total gold load on the surface.

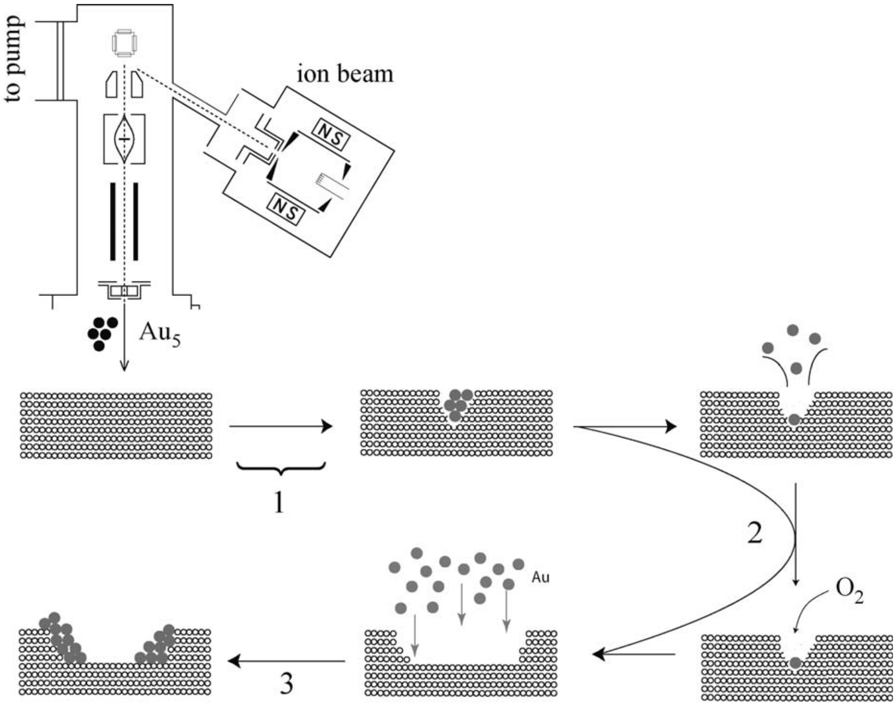

Fig. 1. Schematic representation of the nanostructuring of HOPG consisting in the following three-steps: Au_5 implantation into the atomically clean HOPG surface (1), etching of the created defects under well controlled oxygen partial pressure and temperature (2), gold deposition by thermal evaporation under high vacuum conditions (3).

3. Experiment

Grade-1, highly oriented pyrolytic graphite (HOPG) electrodes used as substrates are provided by *SPI supplies* ®. They exhibit great crystalline perfection (0.4° ± 0.1°). Before surface modification, each HOPG sample is cleaved with adhesive tape resulting in atomically clean terraces containing typically 1–3% step edges. The electrodes are transferred into vacuum immediately after preparation for cluster bombardment.

The cluster source is described elsewhere [29]. Briefly, clusters are produced by sputtering using 20 keV Xe ions extracted from a Cold Reflex Discharge Ion Source (CORDIS). The Xe ions are directed on a sputter gold target. Metal cluster cations are extracted by a series of electrostatic lenses, focused and energy filtered. This filter stops unselected neutrals and performs an energy analysis of the atomic and cluster cations with an energy window of ±7.5 eV. Finally the ions enter a quadrupole mass selector, which allows for mass separation up to 5000 amu. Mass-selected clusters, in this work Au_5, are directed at normal incidence onto the surface. The distribution of deposited clusters on the surface has approximately gaussian shape. The impact energy of the clusters is controlled via a bias voltage applied to the sample. The cluster density is determined by the integrated charge and the cluster beam profile. The densities chosen in these experiments vary between 1000 and 2000 impacts/μm^2.

The etching stage has been performed in a vacuum furnace composed of two chambers, a main chamber and a transfer one, connected together through a valve. A manipulator permits to move the sample forward and back from the transfer chamber to the main one. The furnace allows to reach high vacuum conditions of the order of 10^{-4} Pa. The temperature was fixed to $T = 660\,^{\circ}C$. After temperature equilibration, 8000 Pa clean oxygen was admitted into the furnace. The desired size of the pits is controlled via the exposure time.

Gold deposition has been carried out using two different methods, magnetron sputtering and physical vapor deposition. In order to produce reference samples on unstructured substrates, magnetron sputtering in inert atmosphere at room temperature with a subsequent heat treatment in vacuum conditions (10^{-4} Pa) was used. The deposition rate was controlled via the discharge current and amounts to 0.4 Å s^{-1} corresponding to a material load rate of 2.4×10^{14} atoms $s^{-1}\,cm^{-2}$ or 0.16 ML Au per second. Deposition conditions for different coverages have been kept identical except the exposure time which varied between 1 and 300 s.

For gold deposition on the nanopits substrates, physical vapour deposition has been chosen. The thermal energy of the gold atoms provides, in contrast to the sputtered ones, softlanding conditions without any defect creation on the HOPG surface. Pure gold was evaporated from a molybdenum crucible, heated by direct current flow. The HOPG electrode was kept at $T_s = 400\,^{\circ}$ C to provide enough energy to the incoming gold atoms to diffuse into the created nanopits. The amount of gold deposited was controlled by a quartz microbalance.

The morphology of the sample is determined with a custom built scanning tunneling microscope (STM) operating under constant current conditions. Typical imaging conditions are $U_{gap} = 0.5\,V$ applied to the tip and $I_T = 0.5$ nA. All images were obtained in air at room temperature.

Electrochemical characterization of the samples was performed in a conventional three-electrode cell using a computer-controlled potentiostat (PGstat 30, EcoChemie). The HOPG electrodes with gold deposits were used as working electrode (0.125 cm^2 exposed surface area), $Hg/Hg_2SO_4/K_2SO_4$(sat) as reference electrode and a platinum wire as counter electrode. Solutions were made with ultra-pure water. The characterization method for this type of deposits was cyclic voltammetry in a supporting electrolyte containing no electroactive solute. Cyclic voltammetry has been performed in 0.5 M H_2SO_4 at 25 °C, between the potential limits of 0 and 1.8 V with a scan rate of 100 mV s^{-1}. The voltammetric charge of the reduction of gold oxide was determined by integration of the reduction peak observed in the cathodic scan, typically between 1.3 and 0.8 V. All potentials given are relative to the standard hydrogen electrode (SHE).

4. Results and discussion

Fig. 2 shows a SEM image of a HOPG substrate on which Au was deposited by magnetron sputtering at room temperature. As can be seen most of the particles nucleate at step edges which provide the strongest nucleation sites. Defects which are created by the sputtering process itself provide nucleation centers as well and smaller clusters are observed on the terraces. Clusters which are pinned to the self produced defects on the terraces are less strongly bound than the ones on step edges. This is manifested by the fact that gold clusters are exclusively found on step edges after heat treatment at 400° C under vacuum conditions ($p = 10^{-3}$ to 10^{-4} Pa).

4.1. Structured HOPG surfaces by pit creation

As mentioned in the previous paragraph, gold deposits are unstable on a cleaved HOPG surface. Sputtering deposition results in non-uniform dispersion and size of the gold nanoparticles. This is in contrast to the results obtained on BDD substrates [33]. As this behaviour is not acceptable for any electrocatalytic application, a method to obtain a stable and well-controlled dispersion of gold deposits on HOPG is necessary. Following the result mentioned above that clusters attached to step edges are more stable than the ones attached to defects on the basal plane we intend to increase this stability even further by producing step edges 4 ML height and confine the Au clusters in a nanocontainer. In the following this process is described in more detail.

The first step is to create a defect track on a HOPG terrace by implanting Au_5 at a well defined energy. The choice of the cluster

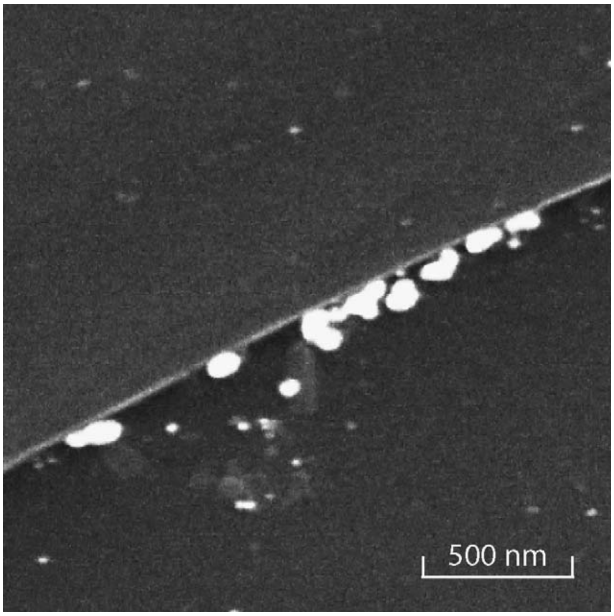

Fig. 2. SEM image of HOPG after Au deposition by magnetron sputtering at room temperature in high vacuum conditions ($p = 10^{-4}$ Pa) followed by a subsequent heat treatment at 400 °C. (Acc.V 10 kV, Magn 2×10^4) size: 2 μm × 2 μm.

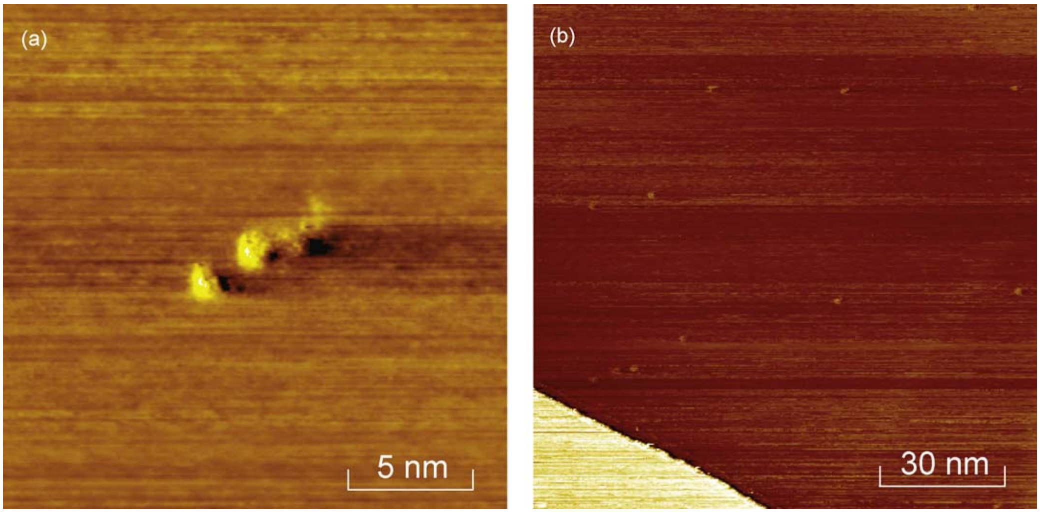

Fig. 3. STM images of two different magnifications of Au_5 clusters implanted in HOPG. Incident kinetic energy: $E_{kin} = 3$ keV; impact density: 1000 μm^{-2}. STM measurements performed at room temperature in air, $U_{gap} = 0.5$ V, $I_T = 0.5$ nA (a: 20 nm × 20 nm, b: 120 nm × 120 nm).

size is a compromise between cluster flux and depth definition. The latter is estimated by the relation given in [36]. For a projected depth of 4 ML in HOPG, the gold clusters containing 5 atoms should possess a kinetic energy of 3 keV.

Fig. 3 shows STM images directly after the implantation step. Cluster induced defects are visible as hillocks (Fig. 3a) which are randomly distributed over the whole surface (bright spots in Fig. 3b). This has already been observed before but usually under ultra high vacuum conditions [28]. Each pit created this way will be an oxidation site during the etching process. This is shown in Fig. 4a. Nanopits from etched Au_5 implanted in HOPG are randomly distributed with negligible overlap which however depends strongly on the pit density. The predicted density from the cluster beam profile and the total deposited charge is well confirmed by the experiment. A histogram showing the distribution of pit diameters is shown in Fig. 4b.

The maximum pit density depends strongly on the mean pit diameter. This diameter can conveniently be varied by the oxidation time. While the pit sizes are rather homogeneous for diameters larger than 20 nm we observe an increasing pit size distribution in the limit to the smallest diameters. This is shown in Fig. 5a. We believe that this is related to the kinetics of the initial etching process. Pits created by oxidation of the HOPG surface have a hexagonal shape following the symmetry of the unit cell. This is shown in Fig. 5a and c. As will be seen below, this particular shape will play a specific role in the nucleation behaviour of gold particles stabilized by the pits. The oxidation is a complex process which implies a cooperative effect divided in two mechanisms. The first one is related to a direct interaction of gas-phase O_2 molecules with the reactive carbon sites (Eley–Rideal mechanism), and the second one involves the reaction of the carbon atoms on the step edges with oxygen which first adsorbs on non reactive sites on the HOPG surface and diffuses to the step edges (Langmuir–Hinshelwood mechanism). Consequently the temperature setting plays a significant role in the etching dynamics. The experimental conditions in this study have been set in a way to favor artificial pits oxidation, which is confirmed by STM measurements (see Fig. 4), and to ensure the desired dimensions of the pits (Fig. 5). Several samples produced under identical experimental conditions have been examined and show a well reproducible pattern of pits with diameters between 10 and 15 nm and depths between 1 and 1.25 nm, corresponding to 4 carbon monolayers.

Gold is deposited into the pits by PVD (physical vapour deposition) under high vacuum conditions. The substrate is heated to $T = 400^\circ$ C to improve diffusion of the gold atoms over the Schwoebel barrier on the rim of the nanopits and to allow them to

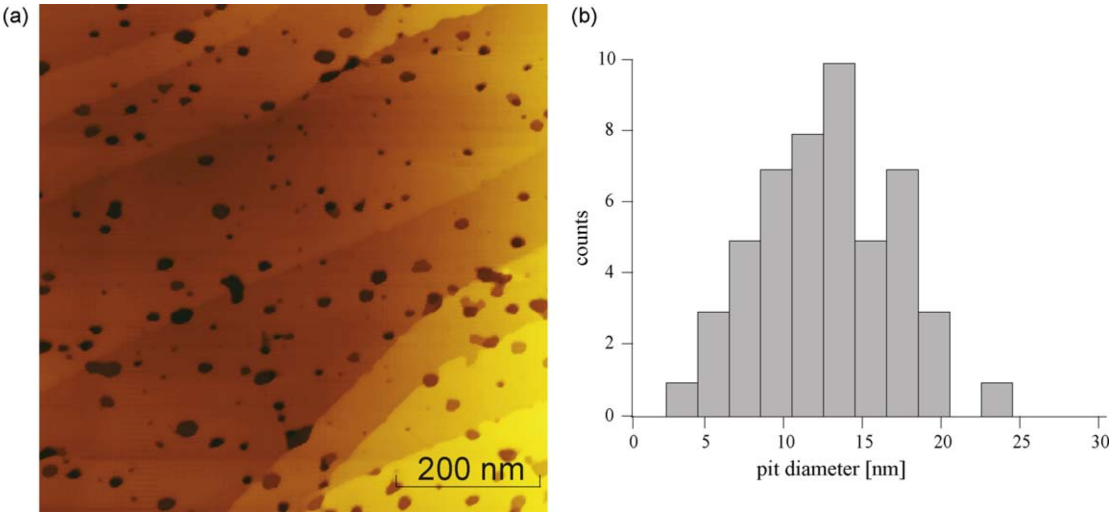

Fig. 4. (a) STM image of HOPG with nanopits (700 nm × 700 nm). Impact density: 2000 μm^{-2}. Etching conditions: $T = 650^\circ$C, $p = 8000$ Pa, $t = 420$ s. STM measurements performed at room temperature in air, $U_{gap} = 0.5$ V, $I_T = 0.5$ nA. (b) Histogram of the size distribution of the etchpits.

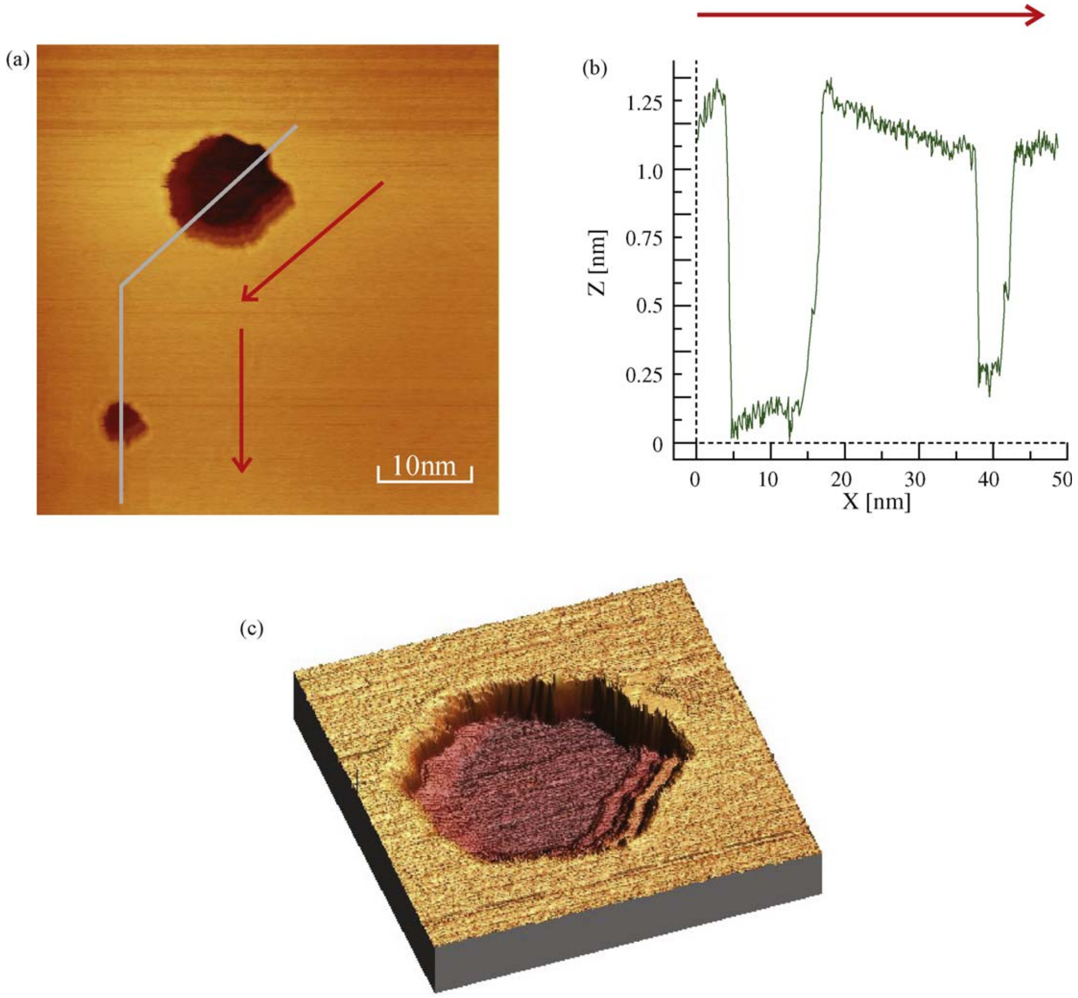

Fig. 5. STM image showing the detail of a nanopit (60 nm × 60 nm). Etching conditions: $T = 650\,^{\circ}\mathrm{C}$, $p = 8000$ Pa, $t = 420$ s. STM measurements performed at room temperature in air, $U_{gap} = 0.5$ V, $I_T = 0.5$ nA. (a) 2D representation, (b) line profile along the trace indicated in (a); 3D representation revealing the depth of 4 ML. Atomic resolution is obtained on the terrace and on the bottom of the pit.

be captured inside the containers. Fig. 6 shows that the gold deposits are located in the containers rather than outside as expected. As mentioned above, pits have a hexagonal form increasing the coordination and consequently the stability of the gold particles when pinned into the corners of the hexagon. This is indeed the case as shown in Fig. 6. As a result most of the containers host 3 larger gold clusters with a typical diameter between 2 and 8 nm depending on the total Au load. The distribution of particle height and diameter is shown in Fig. 6c and d. A detailed analysis of the evolution of the pit size and Au particles size as a function of Au load and deposition conditions goes beyond the scope of this paper and will published in a forthcoming contribution. Smaller structures are discernable in Fig. 6, decorating the rim of the pit. We can, at the moment, not decide whether these particles are made of Au or are impurities attached to the highly reactive dangling bonds. One should keep in mind that the STM images have been taken under atmospheric conditions at room temperature.

4.2. Electrochemical characterization of gold deposits on HOPG surface

The stability of the gold nanostructures has been analyzed by cyclic voltammetry. Sputter deposited gold on unstructured HOPG is compared to PVD deposited gold on nanopit structured HOPG.

A previous study on gold nanoparticles deposited on boron-doped diamond revealed that as-sputtered deposits were unstable under potential cycling in the supporting electrolyte [33]. Stabilization of the Au/BDD electrodes was achieved by a subsequent heat treatment at 600 ° C in air. When using HOPG as a substrate, this method is not directly applicable due to the sensitivity of HOPG to oxidation. In order to avoid surface oxidation of the HOPG substrate, the heat treatment subsequent to sputter deposition performed on a non-structured cleaved HOPG surface was made in vacuum (10^{-3} to 10^{-4} Pa). The temperature was lowered to 400 °C. The stability of such gold deposits on non-structured HOPG surfaces has been evaluated by cyclic voltammetry. The evolution of the voltammograms over continuous cycling is shown in Fig. 7. The charge of the reduction of gold oxide decreases very quickly with the number of cycles. The residual reduction charge after 500 cycles amounts to only 9% of the initial value. Two reasons can explain this loss. First, the gold load suffered losses via corrosion, and second, the active surface decreases due to sintering of individual particles into larger one. SEM analysis (not shown here) has confirmed the decrease in density and the increase in Au particle size after 500 voltammetric cycles. Consequently, sputter deposited Au on non-structured surfaces cannot be considered as stable against potential cycling.

The stability of gold deposits on structured tailored HOPG surface, prepared by physical vapor deposition with simultaneous

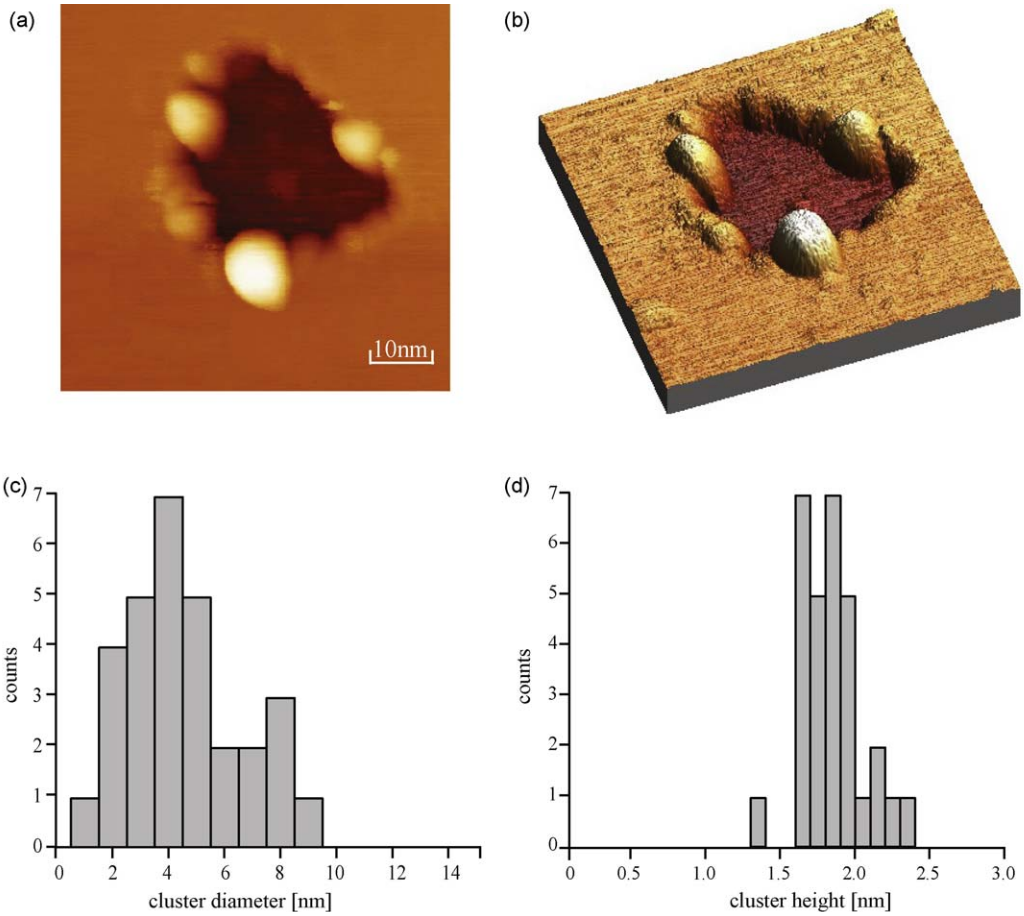

Fig. 6. (a and b) STM image of a nanopit following PVD gold deposition at $T_S = 400^\circ$ C (60 nm × 60 nm). Typically 3 clusters are stabilized per pit. STM measurements performed at room temperature in air, $U_{gap} = 0.5$ V, $I_T = 0.5$ n, (c) histogram of the distribution of cluster diameters found in the pits (corrected for tip convolution effects, (d) histogram of the distribution of Au cluster heights.

heating, has also been studied under voltammetric cycling in the supporting electrolyte. As seen in Fig. 8 for a gold load of 1.8×10^{15} atoms cm^{-2} geometrical surface area, no evolution of CV scans is observed and the reduction peak stays stable over the whole test, indicating a stable morphology and no Au loss. For deposits exceeding 1.8×10^{15} atoms cm^{-2} geometrical surface area, the same behavior has been observed. This stability can be assigned to two main physical reasons: first, the number of gold atoms, enough to build a stable nucleus, and second, the dangling bonds provided inside the pits. Based on the observed stability, we conclude that gold deposits on tailored structured HOPG surface are suitable for electrochemical applications.

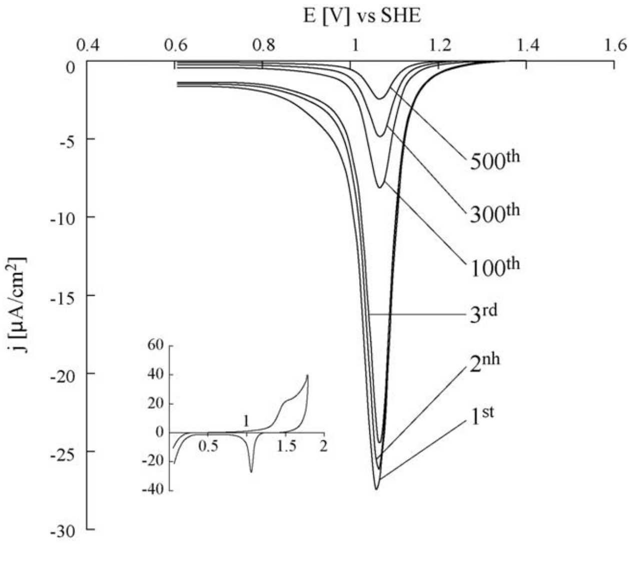

Fig. 7. Evolution of cyclic voltammograms on sputter deposited gold on a nonstructured HOPG substrate (see Fig. 2b) as a function of the number of cycles. Cyclic voltammetry in 0.5 M H_2SO_4 at $T = 25^\circ$C. Scan rate of $S = 100$ mV s^{-1} between the potential limits of 0 and 1.8 V (see inset). Deposited amount: 2.4×10^{15} cm^{-2} gold atoms.

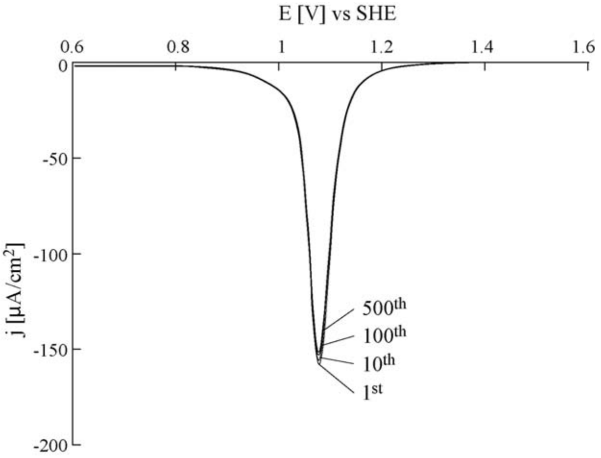

Fig. 8. Evolution of cyclic voltammograms of a gold deposit on a nanopit structured HOPG surface as a function of the number of cycles. Gold amount deposited: 1.18×10^{15} atoms cm^{-2} geometrical surface area. Cyclic voltammetry in 0.5 M H_2SO_4 at $T = 25\,^\circ$C; scan rate $S = 100$ mV s^{-1}; potential limits: 0.6,1.4 V.

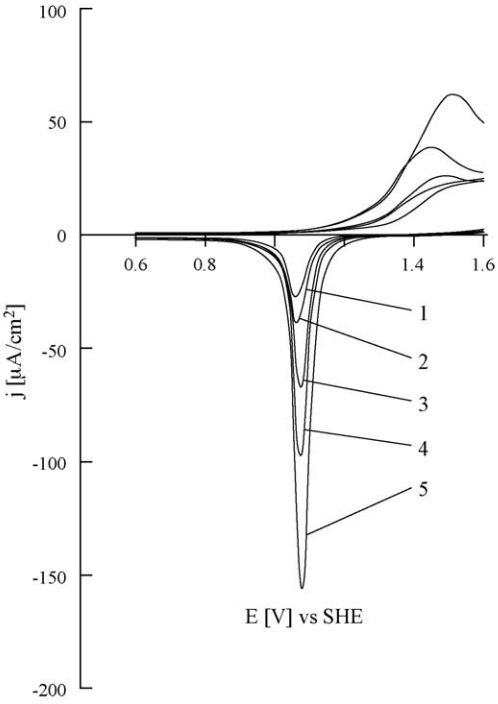

Fig. 9. Evolution of cyclic voltammograms as a function of the amount of deposited gold on a nanopit structured HOPG surface: (1) 3×10^{14} atoms cm^{-2}, (2) 5.9×10^{14} atoms cm^{-2}, (3) 1.2×10^{15} atoms cm^{-2}, (4) 1.8×10^{15} atoms cm^{-2} and (5) 3×10^{15} atoms cm^{-2} geometrical surface area. Cyclic voltammetry in 0.5 M H_2SO_4 at $T = 25\,^{\circ}C$; scan rate $S = 100$ mV s^{-1}; potential limits: 0.05,1.8 V.

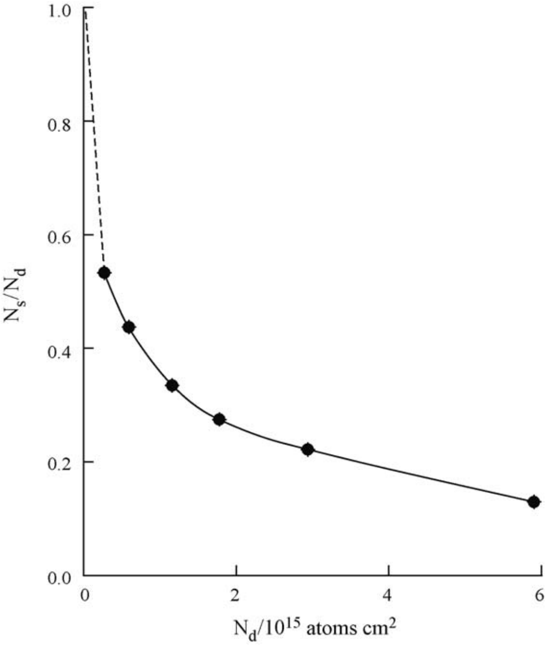

Fig. 10. Dispersion, N_s/N_d, of Au nanoclusters on structured HOPG substrates as a function of the deposited amount, N_d. The density of surface gold atoms, N_s, was calculated from the voltammetric charge of the reduction peak of gold oxide.

The properties of stable deposits depend on several parameters; two of them have been studied in this work: (i) the amount of deposited gold and (ii) the dispersion of such catalyst. For these investigations, a standard procedure has been applied taking the third voltammetric scan in order to ensure electrochemical steady state conditions. Gold nanoparticles of different metal loading have been studied and the CVs are shown in Fig. 9. The peak current response, i_p, increases with metal loading, while the peak potential of gold oxide reduction is rather stable at $E_{red} = 1.08$ V, with exception of gold loadings below 10^{15} atoms cm^{-2} geometrical surface area. The slightly negative shift in the reduction peak potential noticed at such low loadings is probably related to the instability discussed above. On the other hand, increasing the load leads only to an increase of the particle size but not to that of particle density. This is evidenced by looking at the dispersion, N_s/N_d, as a function of metal loading, shown in Fig 10. The number of gold atoms N_s, accessible to the electrolyte and hence active in voltammetry, is only a fraction of the total number of deposited atoms N_d. This fraction decreases as the particle size increases. It can be considered that a new incoming atom would preferentially link to an existing nucleus within a nanopit than create a new nucleus. In fact, the deposition of gold by evaporation on the tailored surface takes place via formation and growth of separate three-dimensional islands and not via completion of successive monolayers.

5. Conclusion

The stability of gold clusters on nanostructured HOPG surfaces has been investigated under electrochemical conditions. The preparation consists in three consecutive steps. In the first step, gold clusters (Au_5) were implanted into the carbon surface in order to create defects of specific depth. In the second step of preparation, nanopits, 4 ML deep and 10 nm in diameter were created by etching under oxygen atmosphere under controlled temperature. Gold from a crucible was evaporated on the substrate under vacuum and well defined temperatures ($T = 400\,^{\circ}C$). A total load of a maximum of 4 monolayers equivalent was deposited. The Au clusters confined in the pits have a diameter of 2–10 nm well in the size region where gold catalysts are supposed to be active and show to be very stable against electrochemical processes. Continuous potential cycling, under usual electroanalytical conditions does not alter the Au/HOPG morphology. We clearly show that even the smooth weakly interacting HOPG surface can be nanostructured to stabilize Au clusters, which means that these electrodes are applicable for electroanalysis studies which are underway.

Acknowledgments

This work has been supported by the Swiss National Science Foundation.

References

[1] G.R. Bamwenda, S. Tsubota, T. Nakamura, M. Haruta, The influence of the preparation methods on the catalytic activity of platinum and gold supported on TiO_2 for co oxidation, Catal. Lett. 44 (1–2) (1997) 83–87.

[2] I. Barke, H. Hovel, Confined shockley surface states on the (1 1 1) facets of gold clusters, Phys. Rev. Lett. 90 (16) (2003), 166801-1, http://dx.doi.org/10.1103/PhysRevLett.90.166801.

[3] J. Berthelot, J. Simonet, Le graphite HOPG: des comportements anodiques et cathodiques particuliers, Electrochim. Acta 29 (9) (1984) 1181–1186, http://www.sciencedirect.com/science/article/B6TG0-44GPH5R-NF/2/86b1aed8a42a6cfeb2791fb8d383da11.

[4] F. Boccuzzi, A. Chiorino, M. Manzoli, Au/TiO_2 nanostructured catalyst: effects of gold particle sizes on co oxidation at 90 K, Mater. Sci. Eng. C 15 (1–2) (2001) 215–217, http://www.sciencedirect.com/science/article/B6TXG-43PBJ3P-1T/2/45bde41b9453878a7037bc776c70d177.

[5] G. Braeuchle, S. Richard Schneider, D. Illig, R.D. Beck, H. Schreiber, M.M. Kappes, Stm investigation of energetic carbon cluster ion penetration depth into HOPG, Nucl. Instr. Meth. B 112 (1996) 105.

[6] G. Brauchle, S. Richard Schneider, D. Illig, J. Rockenberger, R.D. Beck, M.M. Kappes, Etching nanometer sized holes of variable depth from carbon cluster impact induced defects on graphite surfaces, Appl. Phys. Lett. 67 (1) (1995) 52–54.

[7] K. Bromann, H. Brune, C. Felix, W. Harbich, R. Monot, J. Buttet, K. Kern, Hard and soft landing of mass selected Ag clusters on pt(1 1 1), Surf. Sci. 377 (379) (1997) 1051–1055.

[8] K. Bromann, C. Felix, H. Brune, W. Harbich, R. Monot, J. Buttet, K. Kern, Controlled deposition of size-selected silver nanoclusters, Science 274 (5289) (1996) 956–958.

[9] D. Cameron, R. Holliday, D. Thompson, Gold's future role in fuel cell systems, J. Power Sources 118 (1–2) (2003) 298–303, scientific Advances in Fuel Cell Systems. http://www.sciencedirect.com/science/article/B6TH1-48GP6XF-2/2/1932e4f4722d40c427141209ee43d0a6.

[10] S.J. Carroll, S.G. Hall, R.E. Palmer, R. Smith, Energetic impact of size-selected metal cluster ions on graphite, Phys. Rev. Lett. 81 (17) (1998) 3715–3718.

[11] S.J. Carroll, R.E. Palmer, P.A. Mulheran, S. Hobday, R. Smith, Deposition and diffusion of size-selected (ag/sub 400//sup +/) clusters on a stepped graphite surface, Appl. Phys. A 67 (6) (1998) 613–619.

[12] S.J. Carroll, K. Seeger, R.E. Palmer, Trapping of size-selected ag clusters at surface steps, Appl. Phys. Lett. 72 (3) (1998) 305–307.

[14] M.S. El-Deab, T. Sotomura, T. Ohsaka, Oxygen reduction at au nanoparticles electrodeposited on different carbon substrates, Electrochim. Acta 52 (4) (2006) 1792–1798, http://www.sciencedirect.com/science/article/B6TG0-4K0FJT7-4/2/4de39b12dc56be1bdd11db42f2cb4a77.

[15] G. Francis, I. Goldby, L. Kuipers, B. Von Issendorff, R. Palmer, Deposition and growth of noble-metal clusters on graphite, J. Chem, Soc., Dalton Trans. (5) (1996) 665–671.

[16] F. Ghaleh, R. Koster, H. Hovel, L. Bruchhaus, S. Bauerdick, J. Thiel, R. Jede, 2007. Controlled fabrication of nanopit patterns on a graphite surface using focused ion beams and oxidation. J. Appl. Phys. 101 (4), 044301., http://dx.doi.org/10.1063/1.2450677.

[17] Gibilisco, S., Di Vece, M., Palomba, S., Faraci, G., Palmer, R., 2006/08/28. Pinning of size-selected pd nanoclusters on graphite. J. Chem. Phys. 125 (8), 84704-1, http://dx.doi.org/10.1063/1.2337288.

[18] I.M. Goldby, L. Kuipers, B. von Issendorff, R.E. Palmer, Diffusion and aggregation of size-selected silver clusters on a graphite surface, Appl. Phys. Lett. 69 (19) (1996) 2819–2821.

[19] C.-M. Grimaud, R. Palmer, Implantation of pt3- and ag3- clusters into graphite: an stm study, J. Phys.: Condens. Matter 13 (2001) 1869.

[20] J.-D. Grunwaldt, C. Kiener, C. Wögerbauer, A. Baiker, Preparation of supported gold catalysts for low-temperature co oxidation via gold colloids, J. Catal. 181 (2) (1999) 223–232, http://www.sciencedirect.com/science/article/B6WHJ-45GMTGT-C3/2/4dc9b1753eec34793c8121710c6a5278.

[21] J.D. Grunwaldt, M. Maciejewski, O.S. Becker, P. Fabrizioli, A. Baiker, Comparative study of au/tio2 and au/zro2 catalysts for low-temperature co oxidation, J. Catal. 186 (2) (1999) 458–469.

[22] M. Haruta, Size- and support-dependency in the catalysis of gold, Catal. Today 36 (1) (1997) 153–166.

[23] M. Haruta, T. Kobayashi, H.N.Y. Sano, Novel gold catalysts for the oxidation of carbon monoxide at a temperature far below 0 °C, Chem. Lett. 16 (1987) 405–408.

[24] U. Heiz, U. Landman (Eds.), Nanocatalysis, Springer, Berlin, 2007.

[25] H. Hövel, T. Becker, A. Bettac, B. Reihl, M. Tschudy, E.J. Williams, Controlled cluster condensation into preformed nanometer-sized pits, J. Appl. Phys. 81 (1) (1997) 154–158.

[26] M.D. Hughes, Y.-J. Xu, P. Jenkins, P. McMorn, P. Landon, D.I. Enache, A.F. Carley, G.A. Attard, G.J. Hutchings, F. King, E.H. Stitt, P. Johnston, K. Griffin, C.J. Kiely, Tunable gold catalysts for selective hydrocarbon oxidation under mild conditions, Nature 437 (7062) (2005) 1132–1135, http://dx.doi.org/10.1038/nature04190.

[27] T. Irawan, I. Barke, H. Hovel, Size-dependent morphology of gold clusters grown on nanostructured graphite, Appl. Phys. A: Mater. Sci. Process. 80 (5) (2005) 929–935, http://dx.doi.org/10.1007/s00339-004-3118-8.

[28] Jödicke, H., 1999. PhD thesis, EPFL.

[29] H. Jodicke, R. Schaub, A. Bhowmick, R. Monot, J. Buttet, W. Harbich, Deposition of mass-selected clusters studied by thermal energy atom scattering and low-temperature scanning tunneling microscopy: an experimental setup, Rev. Sci. Inst. 71 (7) (2000) 2818–2828.

[30] H. Jodicke, R. Schaub, R. Monot, J. Buttet, W. Harbich, Energetic cluster deposition on a dislocation network: Ag/sub 7/ on 2 ml ag/pt(1 1 1), Surf. Sci. 475 (2001) 1–3.

[31] R. McCreery, Electroanalytical Chemistry, 1990.

[32] S. Pratontep, P. Preece, C. Xirouchaki, R. Palmer, C. Sanz-Navarro, S. Kenny, R. Smith, 2003/02/07. Scaling relations for implantation of size-selected Au, Ag, and Si clusters into graphite. Phys. Rev. Lett. 90 (5), 055503-1, http://dx.doi.org/10.1103/PhysRevLett.90.055503.

[33] B.E. Roustom, G. Foti, C. Comninellis, Preparation of gold nanoparticles by heat treatment of sputter deposited gold on boron-doped diamond film electrode, Electrochem. Commun. 7 (4) (2005) 398–405, http://dx.doi.org/10.1016/j.elecom.2005.02.014.

[34] C. Sanz-Navarro, R. Smith, D. Kenny, S. Pratontep, R. Palmer, 2002/04/15. Scaling behavior of the penetration depth of energetic silver clusters in graphite. Phys. Rev. B 65 (16), 165420-1, http://dx.doi.org/10.1103/PhysRevB.65.165420.

[35] S. Schimpf, M. Lucas, C. Mohr, U. Rodemerck, A. Brückner, J. Radnik, H. Hofmeister, P. Claus, Supported gold nanoparticles: in-depth catalyst characterization and application in hydrogenation and oxidation reactions, Catal. Today 72 (1–2) (2002) 63–78, http://www.sciencedirect.com/science/article/B6TFG-44SK68N-8/2/4954dda50c16180161767e73c3779ccb.

[36] L. Seminara, P. Convers, R. Monot, W. Harbich, Implantation of size-selected silver clusters into graphite, EPJD 29 (1) (2004) 49–56, http://dx.doi.org/10.1140/epjd/e2004-00011-9.

[37] G. Sine, I. Duo, B. El Roustom, G. Foti, C. Comninellis, Deposition of clusters and nanoparticles onto boron-doped diamond electrodes for electrocatalysis, J. Appl. Electrochem. 36 (8) (2006) 847–862, http://dx.doi.org/10.1007/s10800-006-9159-2.

[38] N. Tateishi, K. Nishimura, K. Yahikozawa, M. Nakagawa, M. Yamada, Y. Takasu, Electrocatalytic properties of ultrafine gold particles towards oxidation of acetaldehyde and ethanol, J. Electroanal. Chem. 352 (1–2) (1993) 243–252, http://www.sciencedirect.com/science/article/B6TGB-44XFX33-85/2/6b8a7f957c825612cf3cbc90a1e1d364.

[39] M. Valden, X. Lai, D. Goodman, Onset of catalytic activity of gold clusters on titania with the appearance of nonmetallic properties, Science 281 (5383) (1998) 1647–1650, http://dx.doi.org/10.1126/science.281.5383.1647.

[40] K. Yahikozawa, K. Nishimura, M. Kumazawa, N. Tateishi, Y. Takasu, K. Yasuda, Y. Matsuda, Electrocatalytic properties of ultrafine gold particles supported onto glassy carbon substrates toward formaldehyde oxidation in alkaline media, Electrochim. Acta 37 (3) (1992) 453–455, http://www.sciencedirect.com/science/article/B6TG0-44CH0WY-2C/2/68c288626a3ea5758fe8f69cd3b8a025.

[41] Y. Zhang, S. Asahina, S. Yoshihara, T. Shirakashi, Oxygen reduction on au nanoparticle deposited boron-doped diamond films, Electrochim. Acta 48 (6) (2003) 741–747, http://www.sciencedirect.com/science/article/B6TG0-47TW325-C/2/b54e125d8b6ab5f525cf9d0ac4bb8ef8.